ELSEVIER

Polymer 41 (2000) 1791–1797

polymer

Correct determination of crystal lamellar thickness in semicrystalline poly(ethylene terephthalate) by small-angle X-ray scattering

Z.-G. Wang[a], B.S. Hsiao[a,*], B.X. Fu[a], L. Liu[a], F. Yeh[a], B.B. Sauer[b], H. Chang[c], J.M. Schultz[d]

[a]*Chemistry Department, State University of New York at Stony Brook, Stony Brook, NY 11794-3400, USA*
[b]*DuPont Central Research & Development, Experimental Station, Wilmington, DE 19880-0356, USA*
[c]*DuPont Nylon, Experimental Station, Wilmington, DE 19880-0302, USA*
[d]*Department of Chemical Engineering, University of Delaware, Newark, DE 19716, USA*

Received 19 January 1999; received in revised form 27 April 1999; accepted 30 April 1999

Abstract

For the purpose of resolving an uncertainty over the correct determination of the crystalline lamellar thickness in semicrystalline poly(ethylene terephthalate), PET, via small-angle X-ray scattering (SAXS) analysis, a gel-crystallization method from oligomeric poly-(ethylene glycol) solution was used to prepare samples with high crystallinity (57%). By using simultaneous synchrotron SAXS and wide-angle X-ray diffraction (WAXD) measurements, the heating and cooling processes of the gel-crystallized PET sample were monitored. Results support the assignment of the larger thickness value from the SAXS correlation function analysis as the lamellar crystal thickness. Analysis of WAXD $0\bar{1}1$ reflection line broadening gives the minimum lamellar thickness (in the chain axis) and verifies the thickness assignment for gel and melt crystallized samples. This assignment is critical as it affects the correct interpretation of the crystallization behavior in semicrystalline polymers of relatively low crystallinity.

Keywords: Poly(ethylene terephthalate); Gel crystallization; SAXS

1. Introduction

The behavior of secondary crystallization has been reported in almost all semicrystalline polymers. The secondary crystallization process is frequently used to refer to any effects that can increase the crystallinity after primary crystallization [1]. The nature of secondary crystallization is rather complicated as it may involve the formation of new crystallites with defective structure or smaller thickness, as well as the perfection or thickening of existing crystallites. Recently, we have demonstrated that small-angle X-ray scattering (SAXS) is a useful tool to probe the fundamentals of secondary crystallization in polymers consisting of semi-stiff chains such as poly(ethylene terephthalate) (PET) [2], poly(butylene terephthalate) (PBT) [3] and poly(etheretherketone) (PEEK) [4,5]. However, there is a controversy in the determination of the correct lamellar parameters by SAXS in these polymers due to their relatively low crystallinity ($<$40%) [2–13].

In brief, the controversy over the SAXS analysis stems from the ambivalence of using the correlation function method to determine the crystal thickness [14,15], when the measured polymers have a degree of crystallinity $<$40%. The correlation function analysis can be used to resolve two thicknesses of constituent phases (crystal and amorphous) in the lamellar structure. The analysis, however, cannot determine which thickness represents which phase. Consequently, in the event that the crystallinity is low, one school of researchers inclines to assign the smaller thickness as the crystal thickness. The reason for this is that the product of the long period (L, from SAXS) and the bulk crystallinity (ϕ_c from wide-angle X-ray diffraction (WAXD), differential scanning calorimetry (DSC) or density) is often close to the lower value of the thickness [6,8,9,10]. Such an assignment implies that the resultant morphology consists of space-filled lamellar stacks. Other researchers including us, believe that the opposite assignment is correct for reasons described elsewhere [2–5,7]. According to this assignment, a significant fraction of the material residing outside the lamellar stacks remains in the noncrystalline state. As the calculated two thicknesses in the stacks from the SAXS analysis often exhibit different trends of change with time during crystallization, the opposing assignments often lead to very different interpretations of morphological development during crystallization and

* Corresponding author. Tel.: +1-516-632-7793; fax: +516-632-6518.
E-mail address: bhsiao@notes.cc.sunysb.edu (B.S. Hsiao)

0032-3861/00/$ - see front matter
PII: S0032-3861(99)00327-4

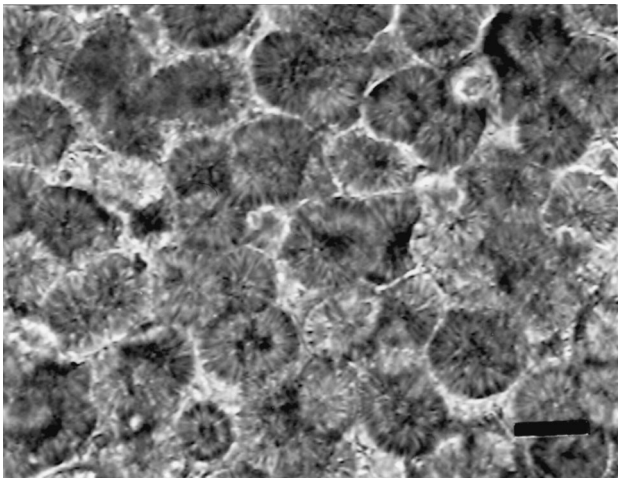

Fig. 1. Optical micrograph of a PET/PEG gel sample with a PET concentration of 20 wt%. The black bar represents 25 μm.

melting of polymers [2–5]. In this paper, we intend to resolve the uncertainty encountered in the SAXS analysis by following the heating and cooling processes of a gel-crystallized PET sample with high initial crystallinity using simultaneous synchrotron SAXS and WAXD techniques.

The method of gel-crystallization to prepare PET samples of high crystallinity (>50%) from concentrate poly(ethylene glycol), PEG, oligomer solutions, has been reported recently [16–17]. An alternative method to obtain the PET sample with high crystallinity (~70%) is by melt-crystallization under high pressure (400 MPa) in the temperature range 295–320°C [18]. In this study, we have used the gel-crystallization method to prepare the sample, as these procedures are relatively simple. Simultaneous synchrotron SAXS and WAXD techniques were used to monitor the lamellar and structural changes during the heating and cooling processes of the gel-crystallized PET sample, which was ideal to resolve the ambivalence of the thickness assignment in the SAXS analysis. This is because as the initial crystallinity is high, there is little question over the determination of the proper lamellar thickness from the SAXS analysis. During heating and cooling processes, as the crystallinity of the samples changes from high to low, the corresponding crystal lamellar thickness can be followed in-situ with temperature. As PET can be viewed as a model system for other polymers containing semistiff chains and relatively low crystallinity (such as polyesters, polyamides and polyetherketones), we hope results from this study may yield information universal to other polymers.

2. Experimental

The PET sample was an experimental grade material provided by DuPont Company, which had a number-average molecular weight (M_n) of 25 000 and a polydispersity (M_w/M_n) of 2. The glass transition temperature T_g and the melting temperature T_m of this sample were 80 and 270°C, respectively. The oligomeric PEG, with a M_n of 400 and T_m of −6°C, was purchased from Aldrich Chemical Company. For the preparation of gel-crystallization, a mixture of 20 wt% PET in PEG was heated to 250°C under rigorous stirring for 10 min to ensure complete dissolution. The homogeneous solution was then cooled at a rate of 10°C/min to room temperature without further agitation to reach a gel state. The final molecular weight of the sample was severely degraded ($M_n = 1060$ and $M_w = 5000$, determined by GPC), perhaps due to high temperature hydrolysis. The melting temperature of the recovered gel-crystallized sample was about 218°C. For the purpose of this study, we feel that the decrease in molecular weight is only of minor importance to the lamellar morphology. The recovered gel-crystallized low molar weight sample is still suitable for the purpose of this study.

The gel specimen containing large fraction of PEG was first examined by a polarized light microscope (Olympus Model BH-2) to observe the spherulite morphology. The gel-crystallized PET sample (in a powder form) was then recovered by repeatedly washing the PET/PEG gel with a large excess of ethanol to remove PEG, and then dried in oven at 80°C for 24 h prior to X-ray measurements. The final sample is free of the PEG component.

Simultaneous synchrotron SAXS/WAXD measurements of the powder gel-crystallized PET sample were carried out at the Advanced Polymers Beamline (X27C, $\lambda = 1.307$ Å) in the National Synchrotron Light Source (NSLS), Brookhaven National Laboratory (BNL). The details of the experimental setup at beamline X27C have been reported elsewhere [19]. Two position sensitive detectors (European Molecular Biological Laboratory, EMBL) were used to detect SAXS and WAXD signals simultaneously. The sample to detector distance for SAXS was 1950 mm and for WAXD was 100 mm. The scattering pattern from silver behenate was used to calibrate the SAXS profile, and isotatic polypropylene (iPP) and silicon standards were used to calibrate the WAXD profile. A custom-made sample chamber was used to heat and cool the sample. An acquisition time of 30 s for each scan was used during heating (from 38 to 274°C at a rate of about 9°C/min) and cooling (from 274 to 110°C at a rate of about 4°C/min).

3. Results and discussion

A typical spherulite-like morphology observed in the PET/PEG gel specimen at room temperature by optical microscopy (without polarization) is shown in Fig. 1. Under cross-polarization, the spherulite morphology is still visible. However, the Maltese cross-extinction patterns, which are characteristic of spherulites grown from the PET melt, are not clear. This observation is different from the

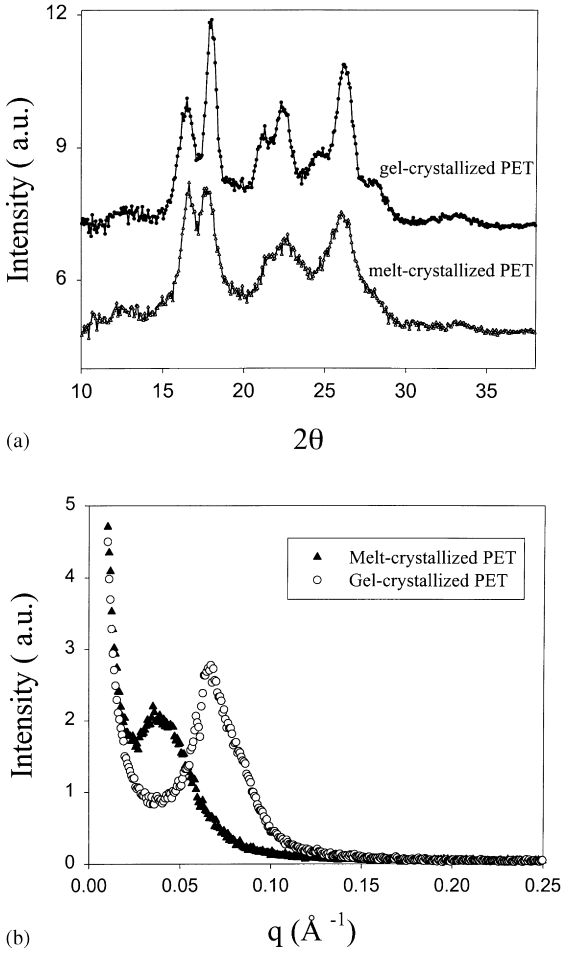

Fig. 2. Simultaneously measured (a) WAXD and (b) SAXS profiles from gel-crystallized and melt-crystallized PET samples.

finding in Ref. [17], where distinct cross-extinction patterns have been reported in the PET/PEG gel. The weak cross-extinction pattern suggests that the local orientation contrast of the moiety in the gel spherulite is low, which may be due to the presence of a large PEG fraction.

Fig. 2(a) and (b) show WAXD and SAXS patterns from the initial gel-crystallized sample (free of PEG) and the final melt-crystallized sample after the cooling process, respectively. From WAXD profiles, it is clear that the peak positions from both samples are almost identical, which indicates a similar unit cell structure. However, the gel-crystallized sample is found to have a much greater degree of crystallinity (57%, this is confirmed by DSC showing 55% crystallinity) than the melt-crystallized sample (40%). The crystallinity was calculated by dividing the sum of the crystalline reflection intensities to the overall intensity. The WAXD deconvolution results, carried out by a curve-fitting program, are shown in Fig. 3. Two Gaussian curves are used to describe the amorphous phase and all crystal reflections (also Gaussian) are separated and indexed. SAXS patterns in Fig. 2(b) indicate that both gel-crystallized and melt-crystallized samples have a lamellar

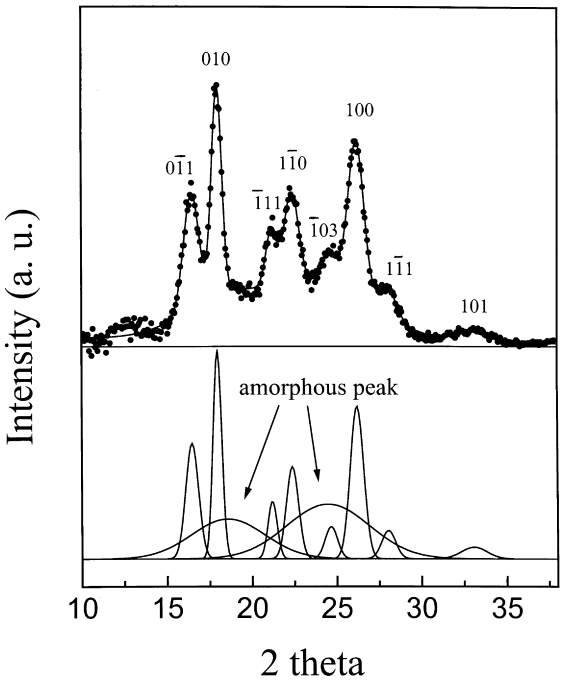

Fig. 3. Peak deconvolution of the WAXD profile from the gel-crystallized PET sample.

structure. The gel-crystallized sample has a long period of 77 Å that is significantly shorter than that of the melt-crystallized sample (118 Å). The higher crystallinity and the denser lamellar structure have also been reported in Ref. [17], which is associated with the high mobility of the chains during crystallization and two steps of gelation processes [17]. We will not discuss the mechanism of gel crystallization here, rather, we will focus on using the gel-crystallized PET sample (with high crystallinity) as a model system to clarify the uncertainty in the SAXS analysis during heating and cooling measurements.

The procedures for calculating the morphological parameters in semicrystalline polymers from the time-resolved SAXS data have been discussed earlier [5,20]. They involve the use of correlation function and interface distribution function to extract parameters such as scattering invariant (Q), long spacing (L) and two thicknesses of the constituent phases (l_1 and l_2, crystal and amorphous thickness). Calculated parameters using the correlation function method only from gel-crystallized PET during heating and cooling processes are shown in Fig. 4. The corresponding crystallinity (X_{mc}) calculated from the WAXD profile is also included in Fig. 4(b). As the initial crystallinity of the sample is high ($X_{mc} = 57\%$), we must assign the larger value (l_1) as the lamellar thickness (l_c), and the smaller value (l_2) as the amorphous layer thickness (l_a). The reasons for this assignment are as follows. As we consider that either l_1 or l_2 may represent the lamellar thickness, we can define the ratio of these values to L as the linear crystallinity within the lamellar stacks. (The linear crystallinity implies that the lamellar stack follows an ideal two-phase model, which has

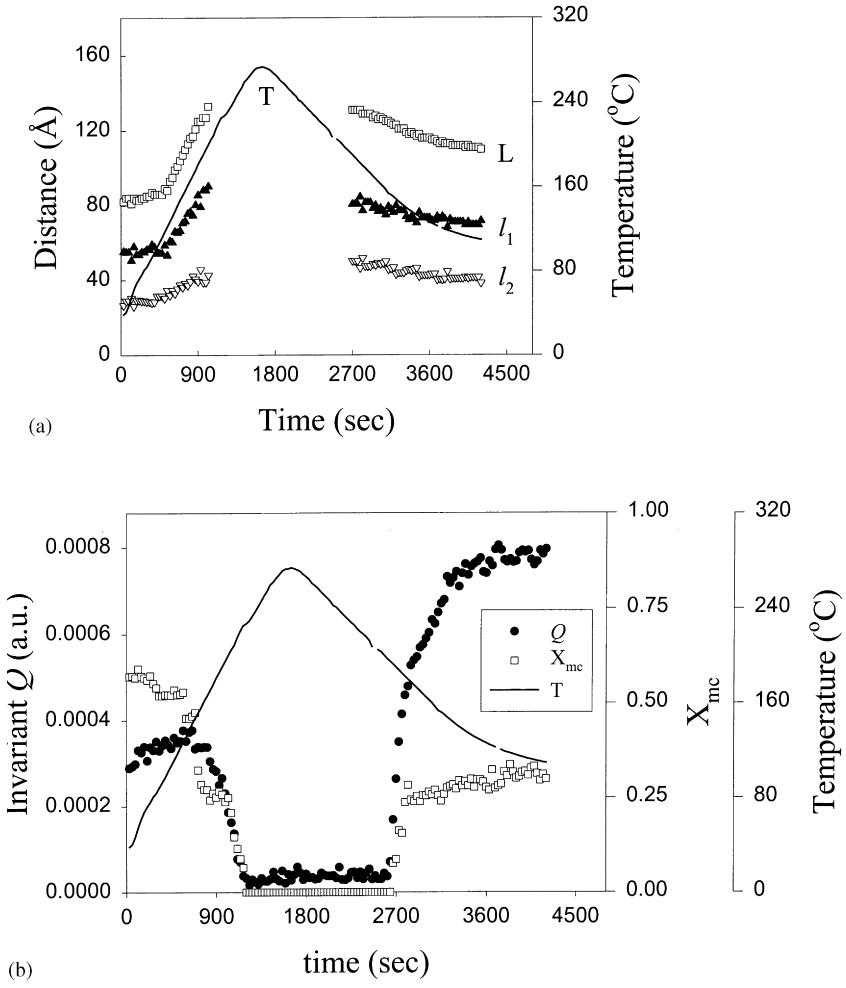

Fig. 4. Time evolution of morphological parameters during heating and cooling processes of powdered PET crystals from PET/PEG gel: (a) long period (L), lamellar thickness, ($l_1 = l_c$) and amorphous layer thickness ($l_2 = l_a$) from SAXS; (b) the invariant (Q) from SAXS and the crystallinity (X_{mc}) from WAXD. (Note that the sample volumes during the heating and cooling processes are not the same.)

a sharp interface between the crystal and amorphous phases.) Moreover, we can define the volume fraction of lamellar stacks (X_{s1} or X_{s2}) in the bulk sample as the ratio of X_{mc} to the linear crystallinity (l_1/L or l_2/L). (We note that the mass degree of crystallinity (X_{mc}) from WAXD is used here instead of the volume degree of crystallinity (X_c). This may be permissible as the density ratio of crystal and amorphous phases in PET is close to the unity.) These results are shown in Fig. 5. In Fig. 5(a), it is interesting to see that both values of l_1/L and l_2/L (linear crystallinity) during heating and cooling are nearly constant, which suggests that the crystal lamellar stack behaves as an integral moiety during the melting and crystallization processes, i.e. the entire stacks melt or crystallize.

In Fig. 5(a), if we assign l_2 as the crystal lamellar thickness, then the values of linear crystallinity (30–40%) will be lower than the bulk crystallinity (>50%) at the initial stage of heating (<110°C or 700 s). This does not make sense because it would suggest that the lamellar stacks fill up more than 100% of the space. In other words, the volume fraction of the lamellar stacks at this stage would be greater than unity as shown in Fig. 5(b), which cannot occur in reality. Thus, the larger value l_1 must be assigned as the crystal lamellar thickness. In this case, the initial volume fraction of the lamellar stacks in gel-crystallized PET is about 90% prior to heating, i.e. the sample is not completely space-filled with lamellar stacks. During cooling when the achievable crystallinity is relatively low (as is usually the case in the literature), both assignments seem possible, which can lead to an uncertainty in the assignment. However, by examining the trends of changes in L, l_1 and l_2, we have to assign the larger value l_1 as l_c. The verification of this assignment can also be made by the further analysis of WAXD data.

Imai et al. have recently reported that the crystal lamellar thickness can be estimated by the crystallite size analysis of the $0\bar{1}1$ reflection peak in the WAXD profile (Fig. 3) [21]. The crystallite size along the c-axis (chain direction), D_{001}, can be calculated from the crystallite size $D_{0\bar{1}1}$ in the direction normal to the lattice plane ($0\bar{1}1$) as shown in Fig. 6. The

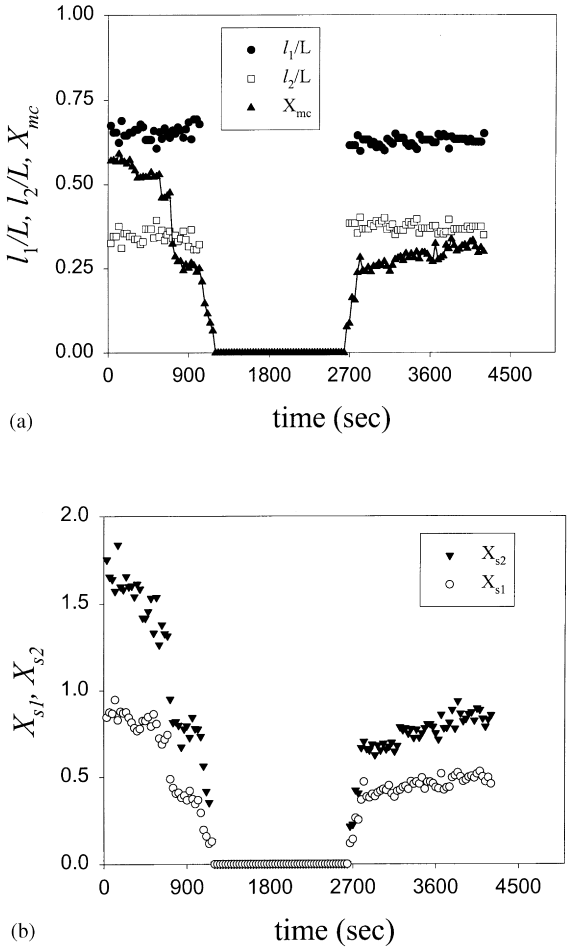

Fig. 5. The changes of (a) linear crystallinity (l_1/L or l_2/L) in the lamellar stacks and bulk crystallinity (X_{mc}), and (b) volume fraction of lamellar stacks (X_{s1} or X_{s2}) during heating and cooling processes of gel-crystallized PET.

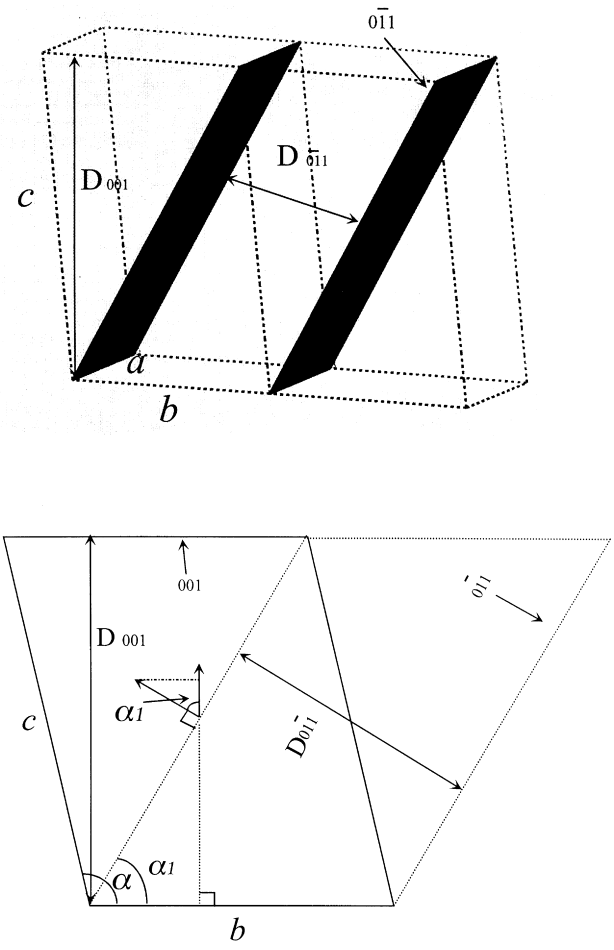

Fig. 6. The schematic diagram of the PET unit cell for calculating the angle between the lattice reflection 001 and $0\bar{1}1$ planes (top) and the projected plane along the *a*-axis (bottom).

two crystallite sizes have the following relationship:

$$D_{001} = D_{0\bar{1}1} \cos \alpha_1 \quad (1)$$

where α_1 is the angle between the (011) and ($0\bar{1}1$) lattice planes. Using the unit cell parameters for the PET crystal ($a = 4.56$ Å, $b = 5.94$ Å, $c = 10.75$ Å, $\alpha = 98.5°$, $\beta = 118°$, $\gamma = 112°$), we can calculate the value of α_1 to be 67.7°. (This value is different from the value reported by Imai et al., who calculated α_1 to be 27°.) As the crystal size $D_{0\bar{1}1}$ can be estimated using the Scherrer equation [22]:

$$D_{0\bar{1}1} = \frac{K\lambda}{\beta_{0\bar{1}1} \cos \theta_{0\bar{1}1}} \quad (2)$$

where K a constant about unity, λ the wavelength, θ the Bragg angle (half of the scattering angle 2θ) and $\beta_{0\bar{1}1}$ the integral breadth of the $0\bar{1}1$ reflection peak. With Eqs. (1) and (2), the crystal lamellar thickness can thus be calculated. Comparisons of values between calculated D_{001} and the two thickness from SAXS (l_1 and l_2) are made in Fig. 7. It is seen that D_{001} agrees well with l_1 in the initial heating stages of the gel-crystallized sample, and D_{001} is consistently larger than l_2 during both heating and cooling processes. As the Scherrer equation always underestimates the true crystallite size, the thickness calculated by Eq. (1) can be viewed as the lower bound (with reasons to be described next) of the crystallite thickness. In this case, we must assign the larger thickness l_1 as the crystal thickness l_c during both heating and cooling processes.

In Fig. 7, we find that the value of D_{001} begins to lag behind l_1 at about 600 s (or 100°C) and l_1 is always larger than D_{001} during cooling. We attribute this behavior to the limitation of using the Scherrer equation to estimate the crystallite size when the thermal motion in the crystals is large during some stages of heating and cooling processes. This is because the thermal vibration about the lattice points in the unit cell can broaden the crystal reflection peak and increase the value of integral breadth; thus the calculated crystallite size can be significantly underestimated by the Scherrer equation. The value of l_1 from SAXS is probably closer to the true value of the crystallite thickness than the value of D_{001} from WAXD. During the initial heating period of the gel-crystallized PET sample, the excellent agreement

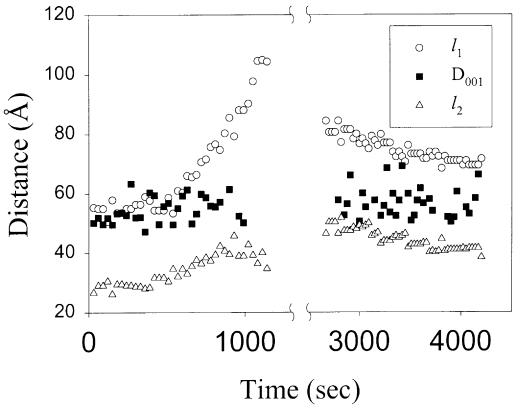

Fig. 7. Comparisons of the values estimated for l_1, l_2 (SAXS) and $D_{0\bar{1}1}$ (WAXD).

between the values of l_1 and D_{001} indicates that the thermal distortion in the initial crystal structure during heating is small.

With the correct assignment of lamellar and amorphous layer thicknesses, changes of morphological parameters with temperature can be explained as follows. During the heating process, both L and l_c ($= l_1$) show a slight increase at the initial stage and a significant increase later on (Fig. 3(a)). The increase in amorphous layer thickness is also visible but with a lesser degree than those of long period and lamellar thickness. The increase in L, l_c and l_a at the initial stage (<110°C) indicates the process of thermal expansion, but the greater change in l_c than l_a suggests that an additional pre-melting process of defective lamellar stacks also exists. These defective lamellar stacks are formed due to nonisothermal crystallization during the cooling process of the gel-crystallized sample. The latter perhaps is a more dominant effect than thermal expansion, which is consistent with the decrease in X_{mc} and the increase in Q (as the contrast increases) (Fig. 4(b)). Above 110°C, we find that all values of L, l_c and l_a increase rapidly and the values of X_{mc} and Q decrease sharply, which suggests that the melting process becomes a dominating factor.

During the cooling process, we find that all values of L, l_c and l_a decrease and the values of Q and X_{mc} increase with decreasing temperature (Fig. 4(a)), which indicates the continuing growth of thinner lamellar stacks. It is known that thinner crystal thickness is produced at lower crystallization temperature [1]. The decrease in temperature should therefore decrease the average values of l_c and L, which is seen. However, the slower change in l_a suggests that the thinner lamellae are probably formed in separate stacks between the existing stacks rather than individual lamellae within the existing stacks. Otherwise, a sharp decrease in l_a is expected, which is not seen. This mechanism is somewhat similar to the dual lamellar stacks model, which has been used to explain the morphology formed by isothermal crystallization [2–5]. The relatively smaller increase in X_{mc} (to only 30%) (Fig. 4(b)) indicates the lack of chain mobility during melt crystallization to achieve a high degree of crystallinity as by gel crystallization. In Fig. 4(b), we note that the value of Q during the cooling process is significantly larger than that during the initial melting process, which is not due to the change in sample structure but due to the increase in sample volume after the melting experiment. This is because the initial volume of the gel-crystallized sample is less because of the large porosity, whereas the volume of the molten sample at the detection position increases after the melting experiment. The values of Q thus cannot be compared between the heating and cooling processes, but they can still be evaluated within the process.

4. Conclusion

In this study, we have used the gel crystallization method to produce a PET sample with lamellar structure and a relatively high crystallinity (57 wt%). The heating and cooling processes of this sample were then followed by simultaneous synchrotron SAXS and WAXD time-resolved measurements. Our objective of this study is to resolve the uncertainty of the SAXS analysis using correlation function to extract the lamellar variables when the bulk crystallinity is relatively low as in most semistiff chain semicrystalline polymers (PET, PBT, PEEK, nylons). We verified that the larger value of the thickness determined by the correlation function analysis of SAXS data should be assigned to the crystal lamellar thickness and the lower value should be assigned to the amorphous interlayer thickness. The results were also verified with the WAXD line broadening analysis of the $0\bar{1}1$ reflection, which gave a minimum lamellar thickness (in the chain axis) as a function of temperature. Finally, we conclude that even with gel crystallization, a small fraction of the material (10%) is still not crystallizable, and the lamellar structure formed by gel crystallization is heterogeneous in nature.

Acknowledgements

The authors acknowledge the financial support of this work by grants from NSF (GOALI-DMR9629825, DMR 9732653), DuPont Young Faculty Grant and DOE funding (DEFG0299ER45760) of the Advanced Polymers Beamline. The authors would also like to thank Haibo Hu and Henry White of Stony Brook for their help of the sample preparation, and Dr David Londono of DuPont for his comments on the WAXD analysis.

References

[1] Wunderlich B. Macromol Phys 1976;2.
[2] Wang ZG, Hsiao BS, Sauer BB, Kampert W. Polymer 1999;40:4615.
[3] Hsiao BS, Wang ZG, Yeh FJ, Gao Y, Sheth K. Polymer 1999;40:3515.
[4] Verma RK, Hsiao BS. Trends Polym Sci 1996;4:9.

[5] Verma R K, Marand H, Hsiao B S. Macromolecules 1996;29:7767.
[6] Medellin-Rodriguez FJ, Phillips PJ, Lin JS. Macromolecules 1996;29:7491.
[7] Santa Cruz C, Stribeck N, Zachmann HG, Balta Calleja FJ. Macromolecules 1991;24:5980.
[8] Groeninckx G, Reynaers H, Berghmans H, Smets G. J Polym Sci, Polym Phys 1980;18:1311.
[9] Medellin-Rodriguez F J, Phillips PJ, Lin JS, Campus R. J Polym Sci, Polym Sci 1997;35:1757.
[10] Jonas AM, Russell TP, Yoon DY. Colloid Polym Sci 1994;272:1344.
[11] Goschel U, Urban G. Polymer 1995;36:3633.
[12] Elsner G, Koch MHJ, Bordas J, Zachmann HG. Makromol Chem 1981;182:1263.
[13] Stribeck N. Colloid Polym Sci 1993;271:1007.
[14] Strobl GR, Schneider M. J Polym Sci, Polym Phys Ed 1980;18:1343.
[15] Vonk CG, Kortleve G. Colloid Polym Sci 1967;220:19.
[16] Xue G, Ji G, Li Y. J Polym Sci, Polym Phys 1998;36:1219.
[17] Xue G, Ji G, Yan H, Guo M. Macromolecules 1998;31:7706.
[18] Balta-Calleja FJ, Ohm O, Bayer RK. Polymer 1994;35:4775.
[19] Hsiao BS, Chu B, Yeh F. NSLS July Newsletter, 1997, 1 (http://bnlx27c.nsls.bnl.gov).
[20] Hsiao B, Verma R. J Synchrotron Rad 1997;5:23.
[21] Imai M, Kaji K, Kanaya T. Macromolecules 1994;27:7103.
[22] Jones FW. Proc R Soc (London) 1938;A166:16.